ÖGH Herpetozoa
Austrian Herpetological Society

Herpetozoa 39: 127–143 (2026)
DOI 10.3897/herpetozoa.39.e188979

Shy highlander: a new species of the genus *Scincella* Mittleman, 1950 (Squamata, Scincidae) from montane forests of Yunnan Province, China

Yuhao Xu[1], Tan Van Nguyen[2,3], Jundong Deng[1], Tierui Zhang[4], Fanyue Sun[1], Junchang Liu[5], Nikolay A. Poyarkov[6], Lifang Peng[1]

1 *State Key Laboratory of Plateau Ecology and Agriculture, Qinghai University, Xining 810016, Qinghai, China*
2 *The School of Medicine & Pharmacy, Duy Tan University, Da Nang 550000, Vietnam*
3 *Center for Entomology & Parasitology Research, Duy Tan University, Da Nang 550000, Vietnam*
4 *Anhui Province Key Laboratory of the Conservation and Exploitation of Biological Resource, College of Life Sciences, Anhui Normal University, Wuhu 241000, Anhui, China*
5 *Fuxing Community, Zhaotong 657799, Yunnan, China*
6 *Department of Vertebrate Zoology, Lomonosov Moscow State University, Leninskiye Gory, GSP–1, Moscow 119991, Russia*

https://zoobank.org/A87D69F0-954E-4E07-AAD0-B4A0D82F2089

Corresponding authors: Lifang Peng (lifang@qhu.edu.cn); Tan Van Nguyen (tan.sifasv@gmail.com); Nikolay A. Poyarkov (n.poyarkov@gmail.com)

Academic editor: Arthur Tiutenko ♦ **Received** 17 February 2026 ♦ **Accepted** 5 April 2026 ♦ **Published** 17 April 2026

Abstract

A new species of the genus *Scincella* Mittleman, 1950, is described from Yunnan Province, China, based on an integrative taxonomic approach combining morphological and molecular evidence. The new species, *Scincella verecunda* **sp. nov.**, is diagnosed by a unique combination of morphological characters, including medium body size in adult females (maximum snout–vent length of 48.7 mm); palpebral disc absent; midbody scale rows 25–26; total ventral + gular scale rows numbering 65–68; paravertebral scale rows 62–65; 6–9 enlarged lamellae beneath finger IV, 11–13 beneath toe IV; in life, the dorsum brown and scattered with a few small dark spots, the lateral surface golden-yellow, bearing numerous distinct dark spots, which sometimes connect to form vermiform markings; the dark dorsolateral stripes irregular; and toes not in contact with fingers when limbs are adpressed. Phylogenetic analyses based on concatenated mitochondrial gene sequences (*12S*, *16S*, and *CO1*) recover the new species as a distinct lineage, forming a clade with *S. ouboteri* Pham, Pham, Le, Ngoc, Ziegler & Nguyen, *S. ochracea* (Bourret), and *S. reevesii* (Gray). The new species status of this population is further supported by marked mitochondrial divergence from its closest relatives (≥ 6.3% in *16S* and ≥ 16.6% in *CO1*) and is currently known only from high-elevation coniferous forest in Linxiang District, Lincang City, Yunnan Province, China (at elevations between 2,113 and 2,358 m a.s.l.). Our data suggest that eyelid morphology may be homoplastic within *Scincella* and that not all *Scincella* species necessarily bear a palpebral disc on the lower eyelid. This finding underlines the need for reconsidering the morphological diagnosis of the genus *Scincella* and allied taxa of sphenomorphine skinks.

Key Words

Lincang City, molecular, morphological characters, taxonomy, *Scincella verecunda* sp. nov.

Copyright *Yuhao Xu et al.* This is an open access article distributed under the terms of the Creative Commons Attribution License (CC BY 4.0), which permits unrestricted use, distribution, and reproduction in any medium, provided the original author and source are credited.

Introduction

The genus *Scincella* Mittleman, 1950, comprises a group of small-bodied, ground-dwelling skinks distributed broadly from Central America through East and Southeast Asia (Ouboter 1986; Zhao et al. 1999; Uetz et al. 2026). Despite their wide geographic range, species diversity within the genus has long been underestimated, largely due to conservative morphology and the prevalence of cryptic lineages. Recent advances in integrative taxonomy, combining molecular phylogenetics with detailed morphological assessments, have dramatically reshaped our understanding of *Scincella* diversity, with a substantial number of new species described over the past few years alone (e.g., Xu et al. 2025a, 2025b, 2025c; Liu et al. 2026; Uetz et al. 2026). These discoveries indicate that many regional faunas remain insufficiently explored, particularly in montane environments. Nevertheless, species boundaries within *Scincella* remain poorly resolved, especially in southwestern China, where complex montane landscapes continue to hide deeply divergent cryptic lineages. Species of *Scincella* are generally characterized by a slender body, well-developed eyelids with a transparent palpebral disc, distinct prefrontals and frontoparietals, an anterior margin of the ear without lobules, a lower secondary temporal overlapping the upper scale, an absence of postnasals and supranasals, a pair of enlarged precloacal scales, and pentadactyl limbs (Mittleman 1950; Ouboter 1986; Greer 1974; Greer and Shea 2003; Nguyen et al. 2010a, 2011). Ecologically, species of the genus occupy a wide range of habitats, from lowland forests and stream margins to rocky slopes and high-elevation montane systems. Such ecological plasticity, combined with subtle interspecific morphological differences, has contributed to persistent taxonomic confusion in several species complexes (Jia et al. 2023, 2024, 2025; Bragin et al. 2025a, 2025b; Nguyen et al. 2025; Xu et al. 2025a, 2025b, 2025c). Southern and southwestern China represent important centers of diversity for the genus *Scincella*, particularly across complex montane landscapes characterized by high habitat heterogeneity. Recent studies have revealed several previously unrecognized lineages from this region, highlighting both its biogeographic significance and the persistent underestimation of local species diversity (e.g., Jia et al. 2025; Xu et al. 2025a, 2025b, 2025c; Liu et al. 2026). These findings suggest that additional undescribed taxa are likely to occur, especially in insufficiently surveyed high-elevation forest ecosystems.

During recent herpetological surveys in high-elevation pine-dominated forests of Lincang City, Yunnan Province, China (Fig. 1), we collected several *Scincella* specimens exhibiting an unusual combination of morphological traits, including the complete absence of a palpebral disc on the lower eyelid. Subsequent comparisons based on external morphology and mitochondrial DNA sequences confirmed that this population represents a distinct evolutionary lineage. Herein, we describe this lineage as a new species of *Scincella* based on an integrative taxonomic framework combining mitochondrial phylogenetics and detailed morphological comparisons.

Materials and methods

Sampling

Six specimens of *Scincella* sp. were collected in Lincang City, Yunnan Province, China. All newly collected specimens were humanely euthanized using a lethal injection of 0.7% tricaine methanesulfonate (MS222) solution, then fixed and stored in 75% ethanol for long-term preservation. Fresh liver tissue was extracted and immediately preserved in 95% ethanol and subsequently stored at –20 °C. All specimens were deposited in the herpetological collection of the museum of Qinghai University, Qinghai Province, China (**QHU**). The related procedures complied with the Wildlife Protection Law of China and were approved by the Institutional Ethics Committee of Qinghai University (protocol number PJ202501-89).

Molecular phylogeny

Total genomic DNA was extracted from preserved liver tissue using the QIAamp DNA Mini Kit (QIAGEN, Changsheng Biotechnology Co. Ltd.). Three mitochondrial gene fragments were amplified: *12S* ribosomal RNA (*12S*) using the primer pair L1091-F (5'-AAACTGGGATTAGATACCCCACTAT-3') and H1478-R (5'-GAGGGTGACGGGCGGTGTGT-3') (Kocher et al. 1989); *16S* ribosomal RNA (*16S*) using *16S*L-F (5'-TGTTTACCAAAAACATAGCCTTTAGC-3') and *16S*L-R (5'-TAGATAGAAACCGACCTGGATT-3') (Linkem et al. 2011); and cytochrome c oxidase subunit I (*CO1*) using RepCOI-F (5'-TNTTMTCAACNAACCACAAAGA-3') and RepCOI-R (5'-ACTTCTGGRTGKCCAAARAATCA-3') (Nagy et al. 2012). Polymerase chain reaction (PCR) amplification followed the protocols described in Jia et al. (2023). The PCR products were sequenced by Shanghai Map Biotech Co., Ltd. Raw sequences were assembled using SeqMan in the DNASTAR software package (Burland 2000). All resulting sequences have been deposited in GenBank under the accession numbers PZ015937–PZ015942 (*12S*), PZ015983–PZ015988 (*16S*), and PZ016030–PZ016035 (*CO1*) (Suppl. material 1: table S1).

In addition to newly obtained sequences, we included 106 sequences from 59 individuals representing 32 nominal *Scincella* species (Suppl. material 1: table S1) and selected *Tropidophorus hainanus* Smith and *T. hangnam* Chuaynkern, Nabhitabhata, Inthara, Kamsook & Somsri as the outgroup (following Bragin et al. 2025b). Three gene fragments, comprising 384 base pairs (bp) of *12S*, 523 bp of *16S*, and 641 bp of *CO1*, were concatenated

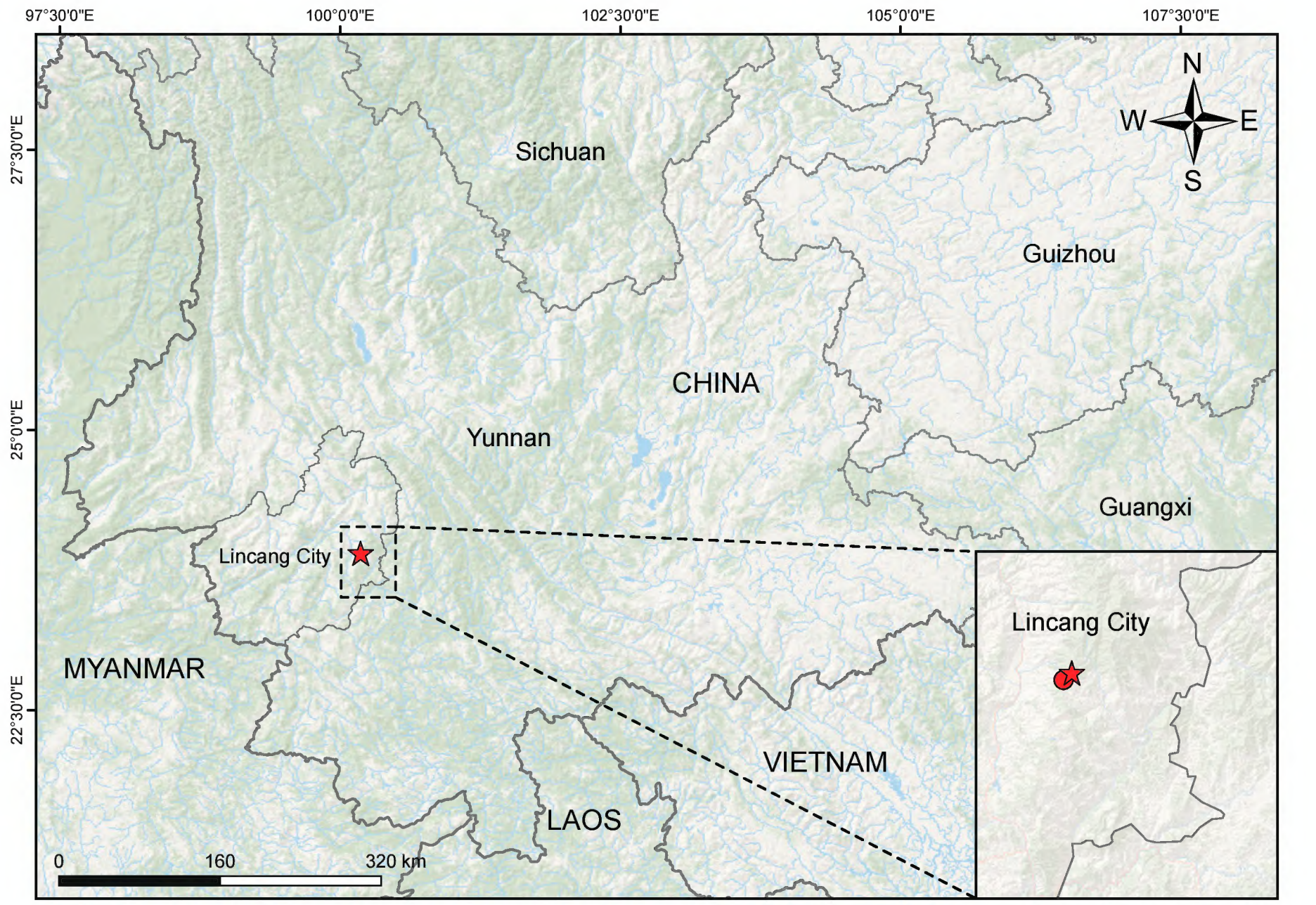

Figure 1. Map showing the locality of *Scincella verecunda* sp. nov. The star indicates the type locality, and the circle denotes another known distribution site.

into a combined dataset (comprising 1,548 bp in total). Sequence alignment was performed using MUSCLE (Edgar 2004) in MEGA X (Kumar et al. 2018). The maximum likelihood (ML) phylogenetic reconstruction was implemented in IQ-TREE v1.6.12 (Nguyen et al. 2015). Substitution models for each mitochondrial gene were determined using ModelFinder as implemented in PhyloSuite v1.2.3 under the Akaike information criterion (AIC) (Zhang et al. 2020; Kalyaanamoorthy et al. 2017; Akaike 1973, 1974). The optimal models selected were TIM2+F+I+G4 for *12S* and *16S*, and GTR+F+I+G4 for *CO1*. Nodal support was evaluated using the SH-like approximate likelihood ratio test (**SH**; 1,000 replicates) and the ultrafast bootstrap method (**UFB**; 5,000 replicates). Nodes with SH values ≥ 80% and UFB values ≥ 95% were interpreted as strongly supported (Stephane et al. 2010; Hoang et al. 2018). The Bayesian inference (BI) analysis was conducted in MrBayes v3.2.7a (Ronquist et al. 2012), with partitions defined by mitochondrial genes. Model selection for BI analyses was performed using ModelFinder for MrBayes in PhyloSuite v1.2.3 under AIC, and the best-fitting model selected for all three gene fragments was GTR+F+I+G4 (Zhang et al. 2020; Kalyaanamoorthy et al. 2017; Akaike 1973, 1974). Three independent Markov chain Monte Carlo runs were executed for 2×10^7 generations, sampling every 1000 generations and discarding the initial 25% of samples as burn-in. Bayesian posterior probabilities (BI PP) ≥ 0.95 were regarded as indicating strong nodal support (Huelsenbeck et al. 2001). Resulting phylogenetic trees were visualized using FigTree v1.4.4 (Rambaut 2018). In addition, uncorrected pairwise genetic distances (*p*-distances) for the *16S* and *CO1* genes between *Scincella* species were also calculated in MEGA X (Kumar et al. 2018) using the uncorrected distance model.

Morphological analyses

Morphological data, including both meristic and morphometric characters, were described following the methodology of Bragin et al. (2025b), with certain character abbreviations revised according to the standards of Darko et al. (2022). Sex was determined by dissection, based on the presence of testes or ovaries. Three morphometric characters were measured using Mitutoyo digital calipers (CD-15AX) and with the naked eye to the nearest 0.1 mm: **SVL** (snout-vent length, measured from the tip of the snout to the posterior edge of vent); **TAL** (tail length, measured from the posterior margin of vent to the

tip of tail); **AGD** (axilla-groin distance, defined as the distance between the posterior edge of the forelimb insertion and the anterior edge of the hindlimb insertion, with both limbs inserted perpendicularly to the body wall). All other measurements were taken using Mitutoyo digital calipers (CD-15AX) to the nearest 0.01 mm under a Leica stereomicroscope (EZ4): **TAW** (tail width, the widest section of tail base); **TAD** (tail depth, measured from ventral to dorsal surface of tail); **MBW** (midbody width, measured from lateral surface to opposing lateral edge at midpoint of the axilla-groin region); **MBD** (midbody depth, measured from ventral surface to dorsal surface at midpoint of the axilla-groin region); **HL1** (head length 1, measured from the tip of the snout to the caudal extremity of the retroarticular process of the mandible, a prominent point externally visible at the posterior end of the lower jaw); **HL2** (head length 2, distance from the tip of the snout to the rear edge of the parietal); **HW** (head width, the widest portion between the left and right articulations of jaw); **HH** (head height, the deepest portion from ventral to dorsal surface of head); **ED** (eye diameter, the length of the palpebral cleft); **END** (eye-narial distance, measured from the anterior corner of the eye to the posterior margin of the naris); **SNL** (snout length, measured from the tip of the snout to the anterior corner of eye); **TD** (tympanum diameter or ear opening diameter, maximum vertical diameter of ear); **EED** (eye-ear distance, distance from posterior margin of eye to anterior margin of tympanum); **IND** (internasal distance, minimum distance between the inner margins of the external nares); **IOD** (interorbital distance, minimum distance between the inner edges of the upper eyelids); **FLL** (forelimb length, measured from anterior junction of forelimb and body wall to tip of the finger IV); **F4L** (finger IV length, measured from the junction between the skin of third and fourth fingers to tip of finger IV); **HLL** (hind-limb length, measured from anterior junction of hindlimb and body wall to tip of toe IV); **T4L** (toe IV length, measured from the junction between the skin of third and fourth toes to tip of toe IV); and **Limbs adpressed** (whether the forelimbs and hindlimbs make contact when the body is held straight and the limbs are adpressed; assessed by calculating the ratio of the sum of forelimb and hindlimb lengths to the axilla-groin length; ratios ≥ 1 indicate that the limbs are able to make contact, whereas ratios < 1 indicate that they are unable to make contact).

Scalation features and their abbreviations were as follows: **SL** (supralabials); **IL** (infralabials); **FrN** (frontonasals); **SCI** (superciliaries); **SO** (supraoculars); **PF** (prefrontals); **FrP** (frontoparietals); **P** (parietals); **PD** (palpebral disc); **TEMP** (enlarged temporals); **Lor** (loreals); **NU** (nuchals); **CS** (chin-shields); **GS** (gulars); **MBSR** (midbody scale rows, number of longitudinal scale rows measured around the widest point of midbody); **PVSR** (paravertebral scale rows, the number of scale rows counted between parietals and the just posterior margin of hindlimbs); **DBR** (dorsal scale rows between dorsolateral stripes, the number of midbody dorsal scale rows between dark dorsolateral stripes); **SRB** (scale rows covered by dorsolateral stripes); **VS** (ventral scale rows, the number of scale rows counted between gulars and precloacals); **F4S** (number of enlarged, subdigital lamellae beneath finger IV); and **T4S** (number of enlarged, subdigital lamellae beneath toe IV).

In addition, following Jia et al. (2024), we also examined the diagnostic coloration characters in *Scincella* species: **UMLLS (**the upper margin of dorsolateral stripes is wavy or relatively straight) and **VDM** (ventral dark markings, the presence or absence of dark-colored markings on the ventral surface).

The comparison with other species of the genus *Scincella* was based on available literature: Gray (1838), Boulenger (1887), Günther (1896), van Denburgh (1912), Stejneger (1925), Barbour (1927), Schmidt (1927), Smith (1935), Bourret (1937), Taylor (1963), Zhao and Huang (1982), Darevsky and Nguyen (1983), Ouboter (1986), Wang and Zhao (1986), Inger et al. (1990), Darevsky and Orlov (1997), Zhao et al. (1999), Chen et al. (2001), Darevsky et al. (2004), Bourret (2009), Nguyen et al. (2010a, b, 2011, 2019, 2020, 2024, 2025), Pham et al. (2015), Neang et al. (2018), Koizumi et al. (2022), Jia et al. (2023, 2024, 2025), Okabe et al. (2024), Pham et al. (2024, 2025), Bragin et al. (2025a, b), Xu et al. (2025a, b, c), and Liu et al. (2026).

Other abbreviations are as follows: **Is** = Island; **Mt**. = Mountain; **NP** = National Park; **NR** = Nature Reserve; and **WS** = Wildlife Sanctuary.

Results

The phylogenetic reconstruction based on concatenated *12S*, *16S*, and *CO1* sequences was largely consistent with recent studies of *Scincella* (Jia et al. 2023, 2024, 2025; Bragin et al. 2025a, 2025b; Xu et al. 2025a, 2025b, 2025c) (Fig. 2). Both ML and BI analyses recovered similar topologies, although most basal nodes remained poorly resolved. Phylogenetic analyses strongly supported the Lincang population as a distinct monophyletic lineage (SH 99 / UFB 100 / BI PP 1.0), recovered as sister to a clade comprising *S. ouboteri* Pham, Pham, Le, Ngoc, Ziegler & Nguyen, *S. ochracea* (Bourret), and *S. reevesii* (Gray) (SH 99 / UFB 100 / BI PP 1.0) (Fig. 2).

The uncorrected *p*-distances, based on *16S* and *CO1* used in this study, are given in Suppl. material 1: tables S2, S3. Uncorrected *p*-distances based on *16S* and *CO1* revealed negligible genetic divergence among specimens from Lincang (0.0–0.5% in *CO1* and 0.0% in *16S*). In contrast, divergences between this lineage and other *Scincella* species ranged from 16.6% (vs. *S. ouboteri*) to 23.2% (vs. *S. melanosticta* (Boulenger)) in *CO1* and from 6.3% (vs. *S. reevesii*) to 11.5% (vs. *S. assata* (Cope)) in *16S*, indicating substantial mitochondrial differentiation. Among *Scincella* species, interspecific *p*-distances ranged from

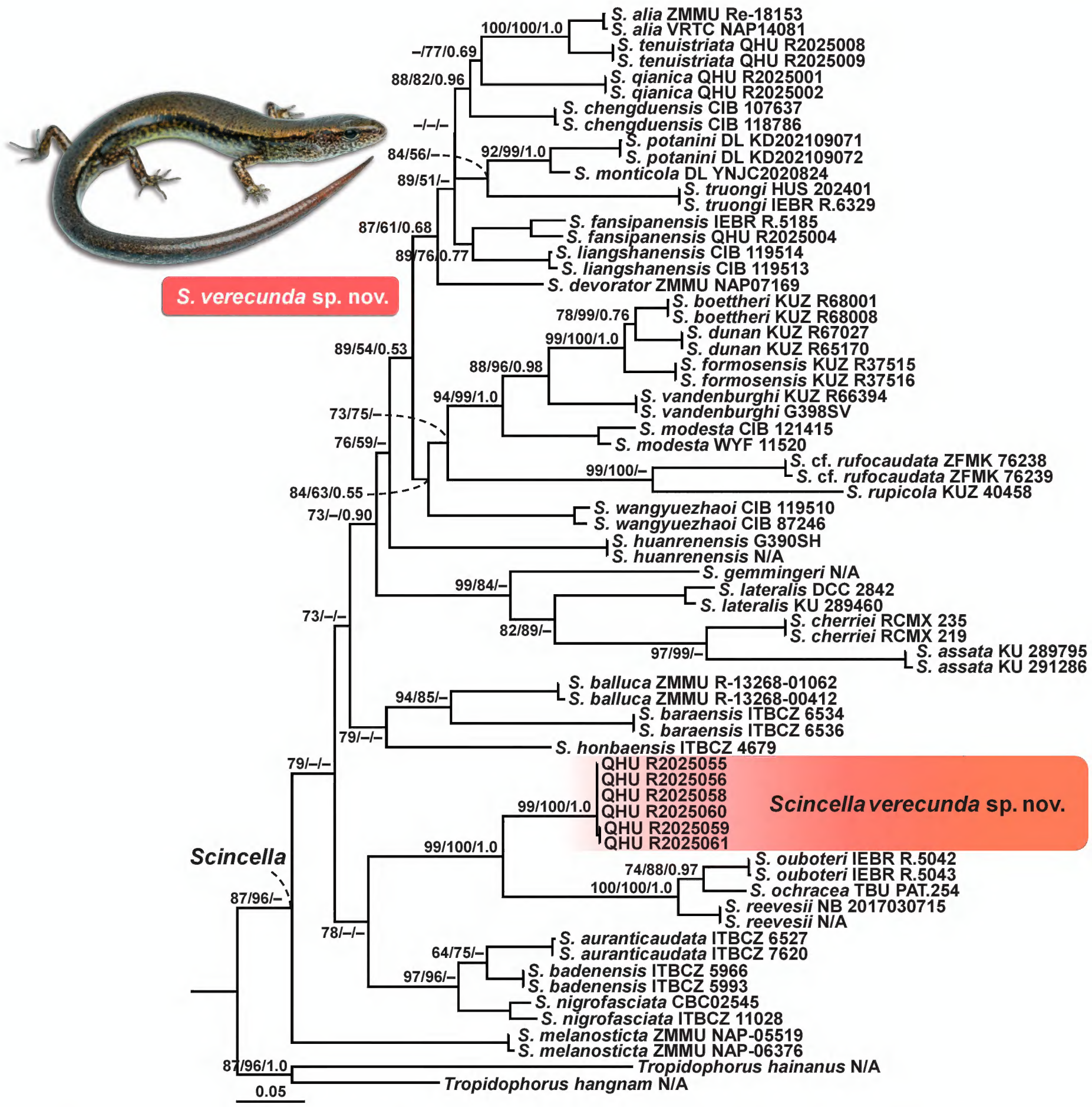

Figure 2. Phylogram of the genus *Scincella* inferred from three mitochondrial (*12S*/*16S*/*CO1*) fragments. The branch support values are presented with the SH-like approximate likelihood ratio test (SH)/ultrafast bootstrap approximation (UFB)/Bayesian posterior probabilities (BI PP); those lower than 50 or 0.5 are displayed as "–". Photograph on thumbnail by Y.H. Xu.

7.6% (between *S. boettgeri* (van Denburgh) and *S. dunan* Koizumi, Ota & Hikida) to 23.4% (between *S. modesta* (Günther) and *S. ochracea*) in *CO1*, with corresponding *16S* divergences ranging from 2.0% (between *S. alia* Bragin, Zenin, Nguyen & Poyarkov and *S. tenuistriata* Xu, Gong, Nguyen, Deng, Bragin, Weng, Zhang, Poyarkov & Peng) to 12.4% (between *S. devorator* (Darevsky, Orlov & Ho) and *S. reevesii*).

Morphological examination revealed a unique combination of scalation characters and body proportions distinguishing the Lincang population from all described congeners (see Taxonomic account below), supporting its recognition as a distinct species, which we formally describe below.

Taxonomic account

Scincella verecunda Xu, Nguyen, Deng, Zhang, Poyarkov & Peng, sp. nov.

https://zoobank.org/40E7FA52-0E05-4861-BDA7-8D9F90DCC727

Tables 1, 2, Figs 3–7

Type material. ***Holotype.*** • QHU R2025058, adult female, from Linxiang District, Lincang City, Yunnan Province, China (23.8977°N, 100.1836°E; elevation 2,358 m a.s.l.) collected by J.D. Deng and Y.H. Xu on 02 July 2025. ***Paratypes* (*n* = 5)**. • QHU R2025059, • QHU R2025061 (two adult females) and • QHU R2025060

(one subadult female), with the same collecting information as the holotype. • QHU R2025055 (one adult female) and • QHU R2025056 (one subadult female) from Linxiang District, Lincang City, Yunnan Province, China (23.8863°N, 100.1697°E; elevation 2,113 m a.s.l.) collected by J.D. Deng and J.C. Liu on 16 June 2025.

Diagnosis. *Scincella verecunda* sp. nov. can be diagnosed from other *Scincella* species by the following unique combination of characters: (1) medium body size in adult female, with a maximum SVL of 48.7 mm; (2) supraciliaries 6–7; (3) supralabials seven, separated from the eye by a row of small scales; (4) infralabials six; (5) palpebral disc absent; (6) midbody scale rows 25–26; (7) ventral scale rows (excluding gulars) 43–45, gulars 20–23, with total ventral + gular scale rows numbering 65–68; (8) dorsal scales smooth, slightly enlarged, with paravertebral scale rows 62–65; (9) toes not in contact with fingers when limbs adpressed; (10) 6–9 enlarged lamellae beneath finger IV, 11–13 beneath toe IV; (11) in life, the dorsum brown and scattered with a few small dark spots, the lateral surface golden-yellow, bearing numerous distinct dark spots, which sometimes connect to form vermiform markings; (12) the dark dorsolateral stripes irregular; and (13) in life, ventral surface of the head creamy white, scattered with small black spots, and the ventral surface of the body golden yellow and immaculate.

Etymology. The specific epithet *verecunda* is derived from the Latin adjective "*verecundus*," meaning "shy" or "retiring." The name refers to the wary disposition and secretive ecological habits of the new species. In the field, individuals rapidly retreated beneath fallen logs or other ground cover when disturbed. Furthermore, the species inhabits remote high-elevation forests above 2,000 m a.s.l. and typically remains concealed within forest-floor microhabitats, making it difficult to detect without deliberate searching. According to its type locality, we suggest the common name "Lincang Ground Skink" in English, "Линьцанский малый сцинк" (Lintsanskiy malyi stsink) in Russian, and "临沧滑蜥" (Pinyin: lín cāng huá xī) as the common name of the new species in the Chinese language.

Description of the holotype. Adult female in good condition. Size medium, SVL 48.7 mm; tail incomplete but relatively long (TaL 81.3+ mm), distal portion regenerated and distinctly narrower than the proximal section; axilla-groin distance 28.9 mm, AGD/SVL ratio 0.59. Head elongated, indistinct from the neck (HL1 9.30 mm, HL2 7.58 mm, HW 5.44 mm, HH 4.27 mm). Snout short, obtuse, round anteriorly (SnL 2.54 mm). Eye large (ED 2.73 mm), lower eyelid without transparent or opaque disc; eye separated from supralabials by a row of small scales. Ear nearly circular; tympanum distinctly, deeply recessed and distinctly without lobules (TD 1.38 mm). Limbs relatively short, toes not in contact with fingers when limbs adpressed (FLL 9.02 mm, HLL 12.16 mm, F4L 1.92 mm, T4L 3.09 mm, FLL/SVL ratio 0.19, HLL/SVL ratio 0.25, FLL+HLL/AGD ratio 0.73). Digits moderately long and slender, each ending in a clearly visible, slightly curved claw. Relative digit lengths of the manus: IV > III > II > V > I, and of the pes: IV > III > V > II > I.

Head scalation **(Fig. 3).** Head scales smooth. Rostral convex, wider than high, distinctly visible from above, in contact with the 1st supralabials, nasals, and frontonasal; supranasals absent; frontonasal one, approximately boat-shaped, width ~2× the height, in contact with the rostral, nasals, anterior loreals, prefrontals, and frontal; prefrontals two, not in contact with each other, separated medially by frontal; frontal slender, longer than wide, diamond-shaped, in contact with the 1st superciliary, 1st and 2nd supraoculars laterally; a pair of frontoparietals, in contact with each other anteriorly, bordered by frontal, 2nd to 4th supraoculars, interparietal, and parietals; interparietal diamond-shaped, width less than height; parietals large, in contact posteriorly, posterolateral border surrounded by the upper secondary temporals and enlarged nuchals; four pairs of enlarged nuchals.

Nostril oval, located at the center of the nasal; nasal entire, diamond-shaped, width approximately equal to height, in contact with the rostral, frontonasal, 1st loreal, and 1st supralabial; loreals 2, subequal in size; supraoculars 4/4, the 1st contacts the frontal, the 2nd is the largest and contacts both the frontal and frontoparietals, and the 3rd and 4th contact the frontoparietal; superciliaries 6/7, the 1st is the largest; the palpebral disc absent; temporals 1+2, the anterior one subrectangular, the upper secondary temporal is the largest, while the lower one is smaller and broadly contacts the upper; supralabials 7/7, 1st smallest, and 6th largest.

Mental wider than long, round anteriorly, in contact with the 1st infralabial and postmental; postmental large and subpentagonal, contacting the mental, the first two infralabials on each side, and the first pair of chin shields; infralabials 6/6, 1st smallest, 5th largest; three pairs of chin shields, the first pair in contact medially, the second pair separated by one gular scale, and the third pair separated by three gulars; gulars 22.

Body scalation **(Fig. 4).** Body scalation smooth, scales around midbody in 26 rows; dorsal scales distinctly larger than lateral scales but nearly equal in size to the ventrals. The paravertebral scale series composed of 64 scales. Dorsal scales between the dorsolateral stripes at midbody 1/2+6+1/2. Ventral scales slightly enlarged medially, decreasing toward the flanks; ventral scale rows (excluding gulars) 45, total GS+VS 67; medial pair of precloacal scales enlarged, the left one overlapping the right one. Tail incomplete; tail scales on the original portion imbricate and generally uniform in shape, except for the markedly widened subcaudals. Limbs pentadactyl; the dorsal surfaces of the fingers and toes covered with two interdigitating rows of scales, with only the two most distal scales single; 7/8 enlarged lamellae beneath finger IV and 11/12 beneath toe IV.

Table 1. Main morphological characteristics of the type series of *Scincella verecunda* sp. nov. All measurements are in mm. The abbreviations of morphological characters are defined in the Materials and Methods section. Notes: ♀ = adult females, S♀ = sub-adult females.

Specimen	QHU R2025058	QHU R2025055	QHU R2025056	QHU R2025059	QHU R2025060	QHU R2025061	*N* = 6
Type	Holotype	Paratype	Paratype	Paratype	Paratype	Paratype	–
Sex	♀	♀	S♀	♀	S♀	♀	
Original tail	No	No	Yes	No	Yes	No	
SVL	48.7	45.1	34.3	47	35.7	43.1	34.3–48.7
TAL	81.3+	48.7+	59.6	56.0+	62.7	44.7+	–
TL	–	–	93.9	–	98.4	–	–
TAL/SVL	–	–	1.74	–	1.76	–	1.74–1.76
TAW	4.33	3.49	2.97	3.56	2.93	3.33	2.93–4.33
TAD	3.65	3.73	2.84	3.42	2.85	3.16	2.84–3.73
AGD	28.88	25.9	18.62	28.54	19.95	25.17	18.62–28.88
AGD/SVL	0.59	0.57	0.54	0.61	0.56	0.58	0.54–0.61
MBW	5.91	4.74	4.09	5.68	3.7	4.15	3.7–5.91
MBD	5.12	3.99	3.3	5.29	3.97	4.12	3.3–5.29
HL1	9.3	9.24	7.83	9.73	8.14	8.57	7.83–9.73
HL2	7.58	7.59	6.26	7.55	6.28	6.97	6.26–7.59
HW	5.44	4.92	4.35	5.07	4.46	5.06	4.35–5.44
HH	4.27	4.01	2.74	4.08	3.27	3.78	2.74–4.27
ED	2.73	2.1	1.89	2.14	1.81	2.02	1.81–2.73
PD	Absent	Absent	Absent	Absent	Absent	Absent	Absent
TD	1.38	1.35	1.11	1.43	1.33	1.44	1.11–1.44
END	1.82	1.93	1.52	1.69	1.61	1.44	1.44–1.93
EED	2.8	2.48	1.93	2.59	2.12	2.6	1.93–2.8
SNL	2.54	2.8	2.3	2.55	2.32	2.33	2.3–2.8
IND	1.67	1.54	1.23	1.23	1.15	1.33	1.15–1.67
IOD	2.88	2.75	2.2	2.51	2.26	2.69	2.2–2.88
FLL	9.02	8.43	7.24	8.5	7.95	8.36	7.24–9.02
HLL	12.16	12.59	9.57	11.78	9.98	11.23	9.57–12.59
FLL/SVL	0.19	0.19	0.21	0.18	0.22	0.19	0.18-0.22
HLL/SVL	0.25	0.28	0.28	0.25	0.28	0.26	0.25-0.28
FLL+HLL/AGD	0.73	0.81	0.90	0.71	0.90	0.78	0.71–0.90
Limbs adpressed	No	No	No	No	No	No	No
F4L	1.92	1.63	1.46	1.61	1.48	1.6	1.46–1.92
T4L	3.09	3.26	2.24	3.17	2.44	2.82	2.24–3.26
MBSR	26	26	26	25	25	26	25–26
DBR	1/2+6+1/2	1/2+6+1/2	1/2+6+1/2	1/2+6+1/2	1/2+4+1/2	1/2+6+1/2	1/2+6 (rarely 4)+1/2
SRB	2–2.5 scales at widest	2–2.5 scales at widest	2–2.5 scales at widest	2–2.5 scales at widest	2–2.5 scales at widest	2–2.5 scales at widest	2–2.5 scales at widest
NU	4/4	4/3	4/3	3/4	4/3	4/3	3–4
PVSR	64	65	62	63	64	64	62–65
VS (Excluding GS)	45	43	45	45	44	45	43–45
GS	22	22	23	20	23	21	20–23
GS+VS	67	65	68	65	67	66	65–68
Lor	2	2	2	2	2	2	2
SL	7/7	7/7	7/7	7/7	7/7	7/7	7
IL	6/6	6/6	6/6	6/6	6/6	6/6	6
Chin	3	3	3	3	3	3	3
SCI	6/7	6/6	6/6	6/6	7/7	6/6	6–7
SO	4	4	4	4	4	4	4
TEMP	1+2/1+2	1+2/1+2	1+2/1+2	1+2/1+2	1+2/1+2	1+2/1+2	1+2
FrN	1	1	1	1	1	1	1
PF	Separated	Separated	Separated	Separated	Separated	Separated	Separated
F4S	7/8	7/7	6/8	8/7	9/8	8/7	6–9
T4S	11/12	12/12	11/11	11/12	13/12	12/11	11–13
UMLLS	Wavy and irregular	Wavy and irregular	Wavy and irregular	Wavy and irregular	Wavy and irregular	Wavy and irregular	Wavy and irregular
VDM	Immaculate	Immaculate	Immaculate	Immaculate	Immaculate	Immaculate	Immaculate

Table 2. Comparison of main morphological characters of *Scincella verecunda* sp. nov., *S. ouboteri*, *S. ochracea*, and *S. reevesii*. Refer to the Materials and Methods for abbreviations of morphological characters. Bold text indicates interspecific diagnostic characters that can be used to distinguish among species.

Species	*S. verecunda* sp. nov.	*S. ouboteri*	*S. ochracea*	*S. reevesii*
SVL (mm)	34.3–48.7	40.9–58.6	34.2–51.0	28.5–58.0
TAL (mm)	–	52.9–76.9	62.3–75.0	36–85
TAL/SVL	**1.74–1.76**	1.09–1.88	–	**1.57–1.70**
AGD (mm)	18.62–28.88	22.0–34.3	26.1–30.0	20.3–24.1
AGD/SVL	0.54–0.61	0.52–0.59	–	–
HL1 (mm)	7.83–9.73	–	–	–
HL2 (mm)	**6.26–7.59**	**7.8–9.5**	–	–
HW (mm)	4.35–5.44	5.4–7.5	–	–
HH (mm)	2.74–4.27	4.0–5.3	–	–
ED (mm)	1.81–2.73	2.2–3.0	–	–
TD (mm)	**1.11–1.44**	**1.5–2**	–	–
SNL (mm)	**2.3–2.8**	**3.5–4.3**	–	–
SNL/SVL	0.05–0.07	0.07–0.09	–	–
FLL/SVL	0.18-0.22	0.22–0.29	0.17–0.27	0.19–0.30
HLL/SVL	**0.25-0.28**	**0.33–0.42**	**0.30–0.38**	**0.34–0.43**
PD	**Absent**	**Present**	**Present**	**Present**
PF	**Separated**	Separated	**In contact**	In contact or separated
SO	4	4	4	4
SCI	6–7	7	7–8	6–9
Lor	2	2	2	2
TEMP	**1+2**	**2+2**	**2+?**	–
SL	7	7	7	7
IL	6	6–7	5–6	6–7
NU	3–4	2–4	0–3	0–3
MBSR	**25–26**	**32**	**30–32**	**28–34**
PVSR	62–65	65–73	61–67	61–77
DBR	**1/2+6 (rarely 4) +1/2**	6	6–8	**8**
GS+VS	65–68	65–71	66–71	63–79
F4S	**6–9**	**10–12**	–	–
T4S	**11–13**	**18–20**	**15–19**	**14–18**
Limbs adpressed	No	Yes	No	Yes or no
Source	This study	Pham et al. (2024)	Bourret (1937); Pham et al. (2015); Neang et al. (2018)	Smith (1935); Zhao et al. (1999); Chen et al. (2001); Neang et al. (2018)

Coloration of the holotype in life **(Fig. 5).** In life, dorsal surface of the head brown, bearing several small, irregular black spots. Upper half of lateral head brown, gradually fading ventrally to light brown, densely marked with relatively large, irregular black spots. Dorsal surfaces of body and tail brown, with a few scattered black spots. A generally broad, dark dorsolateral stripe present on trunk, wavy in outline with highly irregular margins; width variable, occupying approximately 0.5 scale at narrowest point and up to 2.5 scales at widest. The stripe originates at the tip of the snout, extends along the upper margins of the nasal and loreal scales, is interrupted at the eye, reappears posterior to the eye, and continues along the flanks above the forelimbs and hindlimbs to the mid–posterior portion of the tail.

Ground color of flanks light golden yellow, densely marked below the dorsolateral stripe with relatively large, irregular black spots; these spots sometimes confluent or connected to the dorsolateral stripe, forming vermiform patterns in some areas of the flanks. Black markings gradually disappear toward the ventral margin.

Ventral surface of head creamy white; lateral portions of head venter with several black spots, decreasing medially. Ventral surface of trunk golden yellow, immaculate. Anterior portion of tail venter yellow, gradually transitioning posteriorly to gray; gray region densely covered with small dark spots.

Coloration of the holotype in preservation **(Fig. 6).** After seven months in ethanol, the dorsal coloration remains similar to that in life, although the luster is reduced. The golden yellow on the flanks and ventral surfaces has faded to grayish white, but the dark markings remain distinct.

Variation. Morphometric and meristic data of the type series of *Scincella verecunda* sp. nov. are provided in Table 1. The paratypes exhibit coloration generally similar to the holotype, with minor individual variation (Figs 5, 7). The main differences in morphometric and

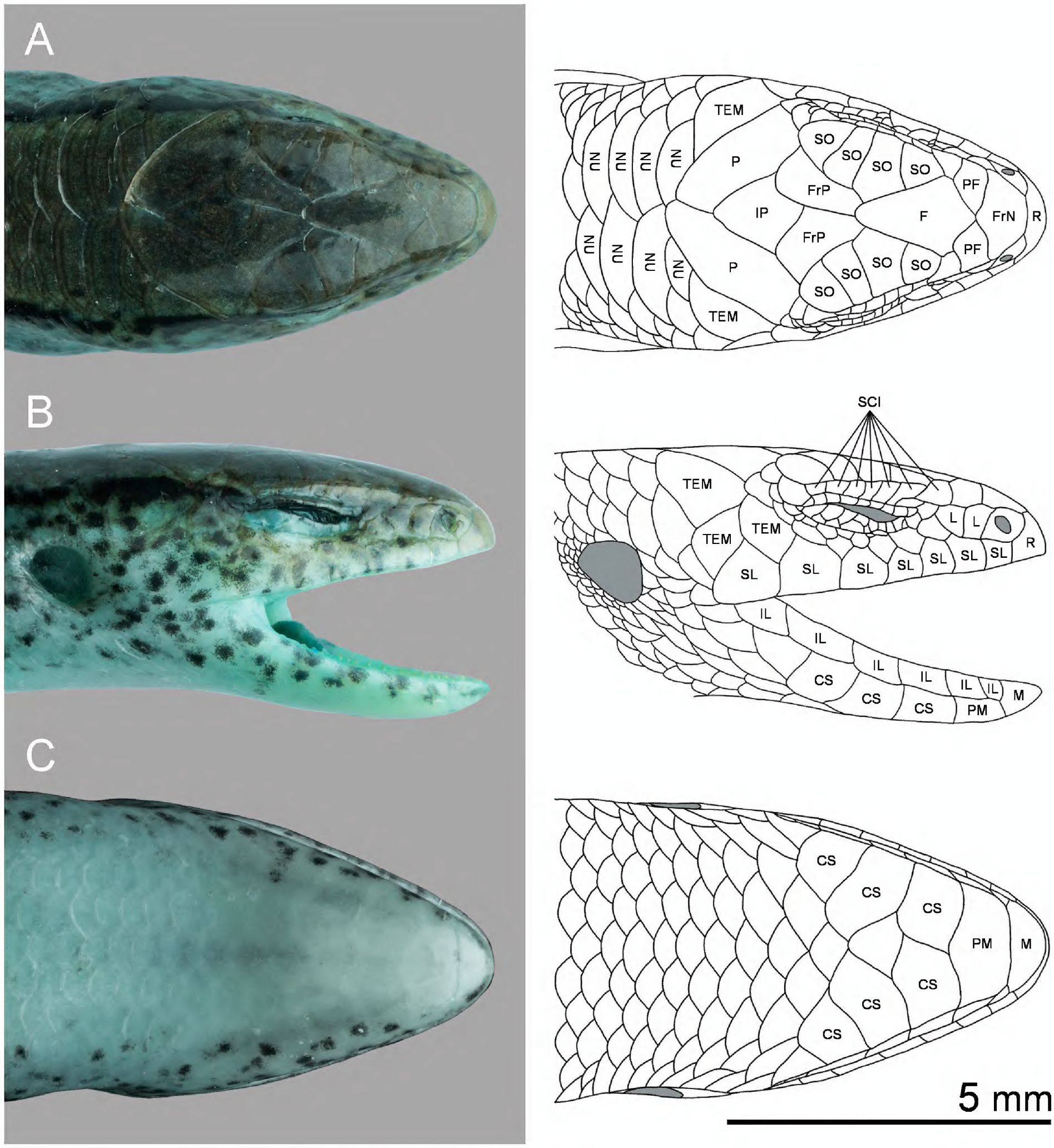

Figure 3. Head scalation of *Scincella verecunda* sp. nov. (holotype, QHU R2025058, adult female). **A.** Dorsal; **B.** Lateral; **C.** Ventral views. Notes: CS: chin-shield; F: frontal; FrN: frontonasal; FrP: frontoparietal; IL: infralabials; IP: interparietal; L: loreals; M: mental; NU: nuchals; P: parietal; PF: prefrontal; PM: postmental; R: rostral; SCI: supraciliaries; SL: supralabials; SO: supraoculars; TEM: temporals. Photographs and drawings by Y.H. Xu. Scale bar: 5 mm.

scalation characters among the type series (N = 6, all females) are as follows: (1) in the two specimens with original tails, TAL/SVL ratio 1.74–1.76; (2) in QHU R2025059, a small, separate scale is split off from the left anterior corner of the frontal scale; (3) MBSR 25–26; (4) SCI 6–7; (5) DBR 1/2+6+1/2, except in QHU R2025060, in which DBR is 1/2+4+1/2; (6) PVSR 62–65; (7) VS 43–45, GS 20–23, VS+GS 65–68; and (8) F4S 6–9, T4S 11–13.

Distribution and natural history notes. At present, *Scincella verecunda* sp. nov. is known only from two closely adjacent localities in Linxiang District, Lincang City, Yunnan Province, China (Fig. 1). Within this area, the new species inhabits high-elevation coniferous or coniferous and broad-leaved mixed forests at elevations of 2,113–2,358 m a.s.l. (Fig. 8A). The forest floor is characterized by a thick layer of pine-needle litter and abundant moss cover, with numerous fallen logs providing additional mi-

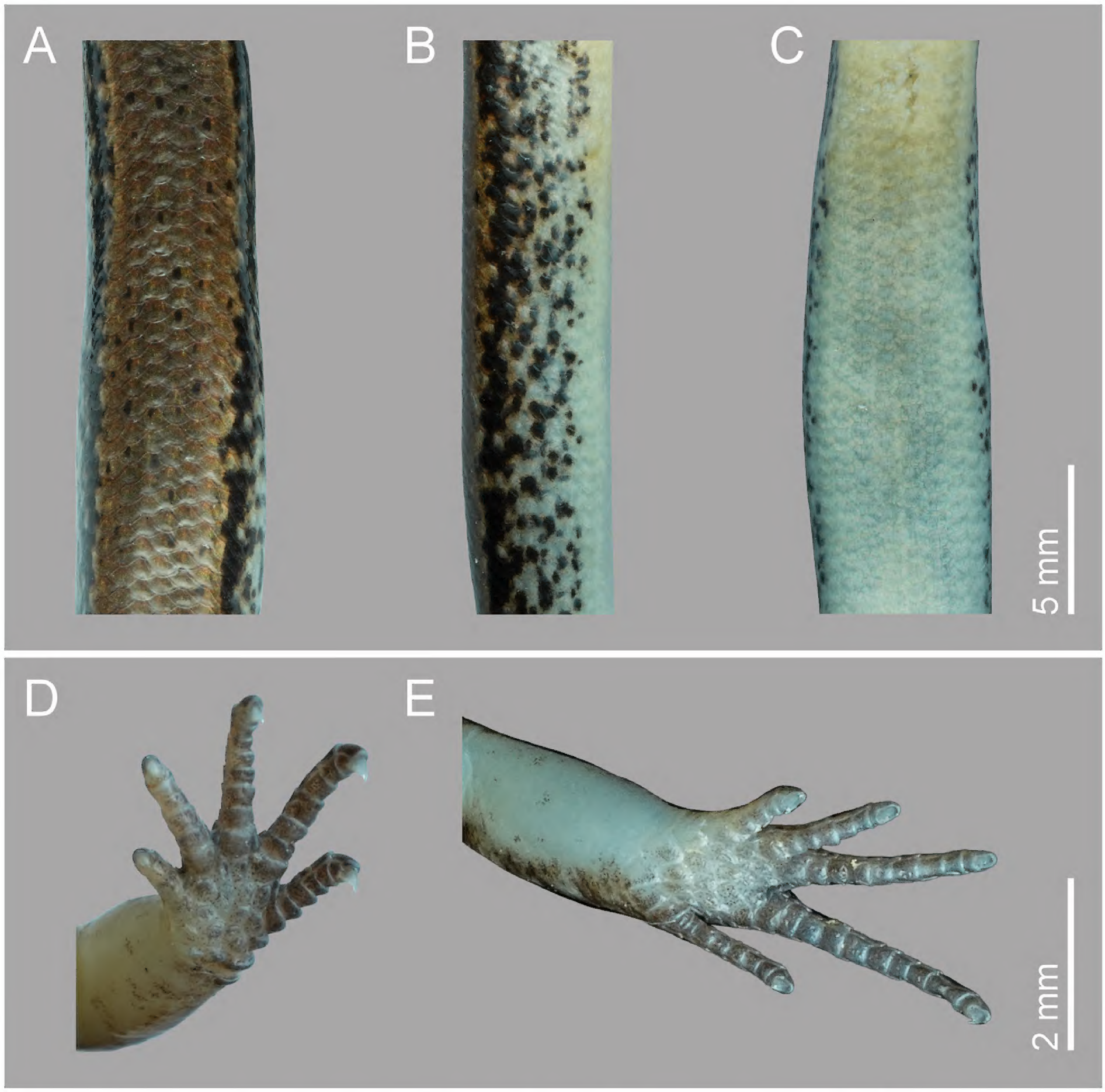

Figure 4. Dorsal (**A**), lateral (**B**), and ventral (**C**) views of the body; **D.** Ventral view of the hand; **E.** Ventral view of the foot of *Scincella verecunda* sp. nov. (holotype, QHU R2025058, adult female) in preservation. Photographs by Y.H. Xu. Scale bars: 5 mm (**A–C**); 2 mm (**D, E**).

crohabitats (Fig. 8B, C). Individuals were observed active on the ground surface from daytime until dusk (Fig. 8D). During the survey period, daytime air temperatures ranged from 20–24 °C, with frequent rainfall and generally high ambient humidity. Given the geographic proximity and continuity of montane habitats, the species may potentially occur in adjacent areas of northern Myanmar.

Conservation status. Field surveys indicate that *Scincella verecunda* sp. nov. is commonly encountered at its currently known localities. However, the limited information available suggests that it is more closely associated with well-preserved, high-elevation montane primary forests. Given the lack of comprehensive data on its overall distribution, population trends, and potential threats, we provisionally assign this species to Data Deficient (DD) under the IUCN Red List Categories and Criteria (IUCN 2026). Additional field surveys and ecological studies are required to better define its range and to enable a more rigorous assessment of its conservation status.

Comparisons. Based on molecular evidence, *Scincella verecunda* sp. nov. is most closely related to *S. ouboteri*, *S. ochracea*, and *S. reevesii*. Detailed morphological comparisons between *Scincella verecunda* sp. nov. and its closely related congeners are provided in Fig. 9 and Table 2. However, *Scincella verecunda* sp. nov. can be readily distinguished from *S. ouboteri* by: (1) palpebral disc absent (vs. present); (2) smaller HLL/SVL ratio (0.25–0.28 vs. 0.33–0.42); (3) temporals 1+2 (vs. 2+2); (4) fewer midbody scale rows (MBSR 25–26 vs. 32); and (5) fewer subdigital lamellae under the fourth finger (F4S

Figure 5. Dorsal (**A1, B1**) and ventral (**A2, B2**) views of *Scincella verecunda* sp. nov. in life. **A1, A2.** QHU R2025058, holotype, adult female; **B1, B2.** QHU R2025055, paratype, adult female. Photographs by Y.H. Xu.

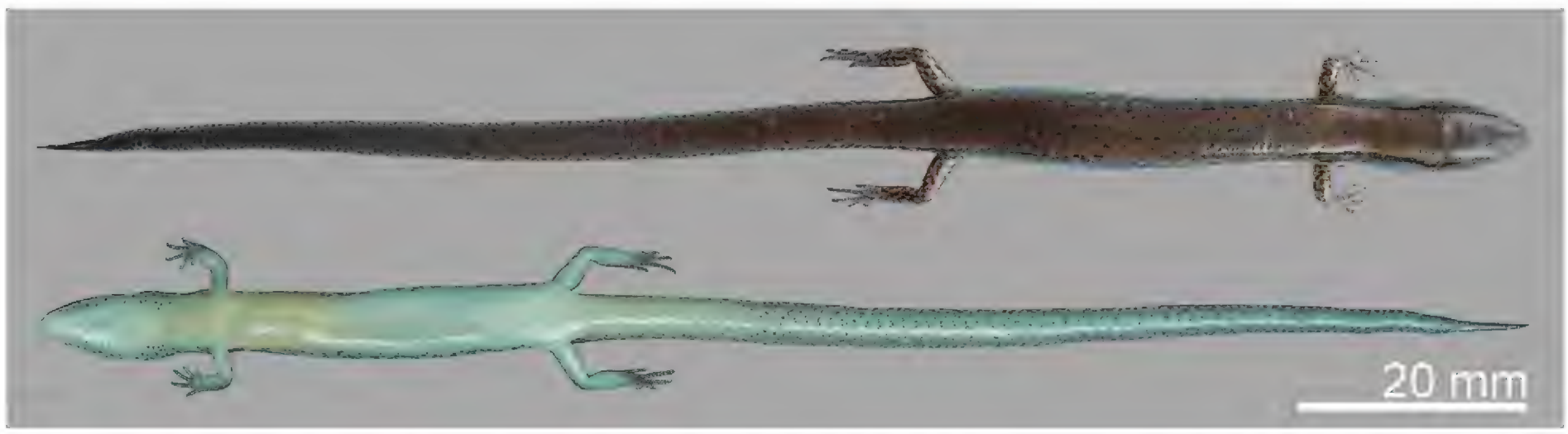

Figure 6. Dorsal and ventral views of the holotype (QHU R2025058, adult female) of *Scincella verecunda* sp. nov. in preservation. Photographs by Y.H. Xu. Scale bar: 20 mm.

6–9 vs. 10–12) and fourth toe (T4S 11–13 vs. 18–20). The new species can be distinguished from *S. ochracea* by (1) palpebral disc absent (vs. present); (2) smaller HLL/SVL ratio (0.25–0.28 vs. 0.30–0.38); (3) prefrontals separated (vs. in contact); (4) one anterior temporal (vs. two); (5) fewer MBSR (25–26 vs. 30–32); and (6) fewer T4S (11–13 vs. 15–19). It can further be distinguished from *S. reevesii* by (1) palpebral disc absent (vs. present); (2) relatively longer tail (TAL/SVL 1.74–1.76 vs. 1.57–1.70); (3) smaller HLL/SVL ratio (0.25–0.28 vs. 0.34–0.43); (4) fewer MBSR (25–26 vs. 28–34); and (5) fewer T4S (11–13 vs. 14–18).

In addition, the absence of a palpebral disc readily distinguishes *Scincella verecunda* sp. nov. from all other currently recognized Asian congeners, including *S. alia*, *S. apraefrontalis* Nguyen, Nguyen, Böhme & Ziegler, *S. auranticaudata* Nguyen, Nguyen, Le, Nguyen, Phan, Vo, Murphy & Che, *S. badenensis* Nguyen, Nguyen, Nguyen & Murphy, *S. balluca* Bragin, Zenin, Le, Nguyen, Nguyen, Bobrov & Poyarkov, *S. baraensis* Nguyen, Nguyen, Nguyen & Murphy, *S. barbouri* (Stejneger), *S. boettgeri*, *S. chengduensis* Jia, Gao, Wu, Wang, Liu, Liu, Jiang, Jiang, Ren & Li, *S. darevskii* Nguyen, Ananjeva, Orlov, Rybaltovsky & Böhme, *S. devorator*, *S. doriae* (Boulenger), *S. dunan*, *S. fansipanensis* Okabe, Motokawa, Koizumi, Nguyen, Nguyen & Bui, *S. formosensis* (Van Denburgh), *S. heishuiensis* Liu, Pu, Tan, Chen, Lyu, Shu, Wu, Dong, Guo, *S. honbaensis* Nguyen, Nguyen, Le, Nguyen, Phan, Vo, Murphy & Che, *S. huanrenensis* Zhao & Huang, *S. incerta* (Stuart), *S. liangshanensis* Jia, Gao, Wu, Ren, Jiang & Wu, *S. melanosticta*, *S. modesta*, *S. monticola* (Schmidt), *S. nigrofasciata* Neang, Chan & Poyarkov, *S. potanini* (Günther), *S. przewalskii* (Bedriaga), *S. punctatolineata* (Boulenger), *S. qianica* Xu, Weng, Poyarkov, Zhang, Deng & Peng, *S. rara* (Darevsky & Orlov), *S. rufocaudata* (Darevsky & Nguyen), *S. rupicola*

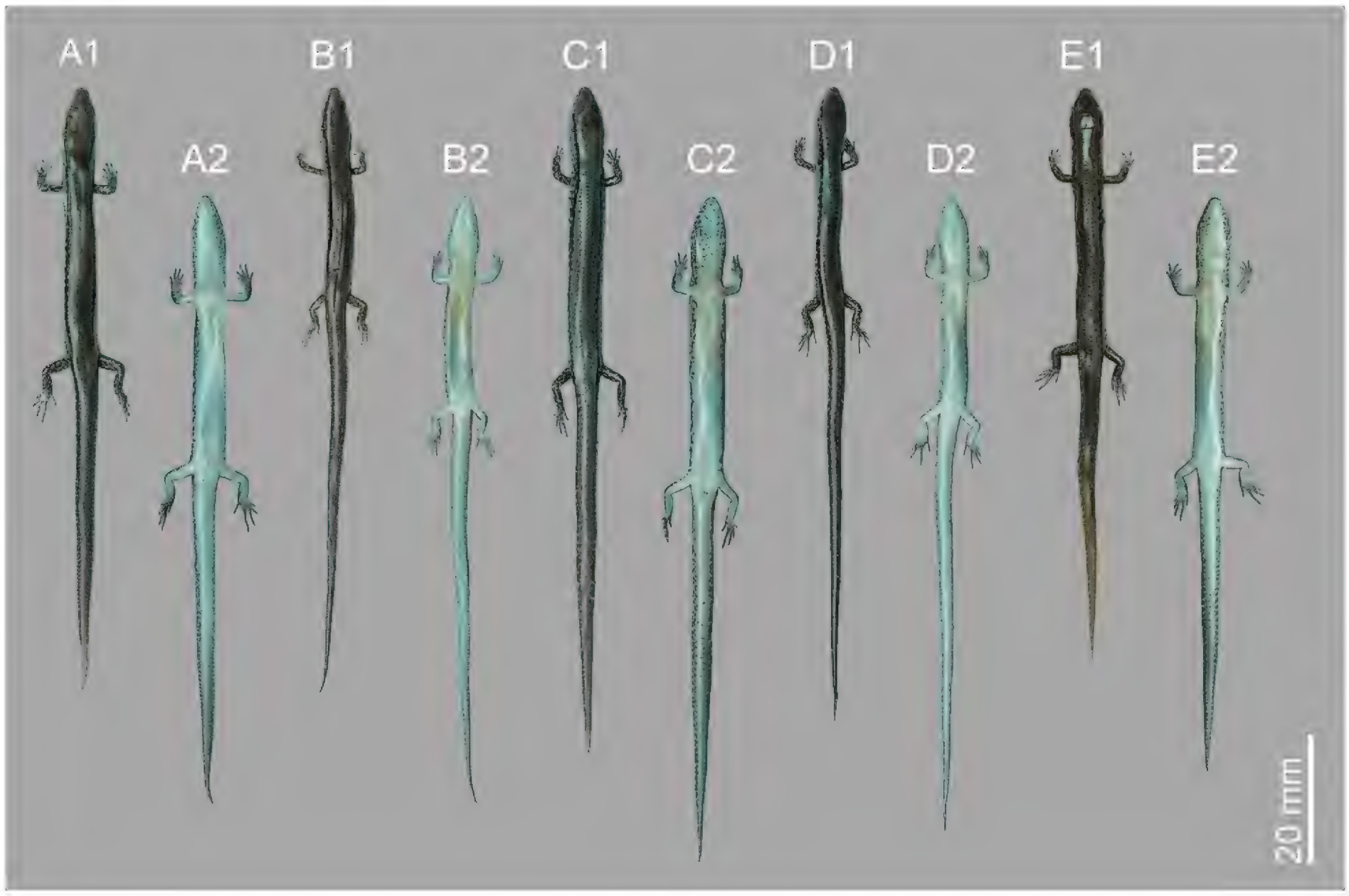

Figure 7. Preserved paratypes of *Scincella verecunda* sp. nov. **A1–E1**. Dorsal views; **A2–E2**. Ventral views. **A1, A2.** QHU R2025055, adult female; **B1, B2.** QHU R2025056, subadult female; **C1, C2.** QHU R2025059, adult female; **D1, D2.** QHU R2025060, subadult female; **E1, E2.** QHU R2025061, adult female. Photographs by Y.H. Xu. Scale bar: 20 mm.

(Smith), *S. schmidti* (Barbour), *S. tenuistriata*, *S. truongi* Pham, Ziegler, Pham, Hoang, Ngo & Le, *S. tsinlingensis* (Hu & Zhao), *S. vandenburghi* (Schmidt), *S. victoriana* (Shreve), and *S. wangyuezhaoi* Jia, Gao, Huang, Ren, Jiang & Li (vs. present).

Discussion

The discovery of *Scincella verecunda* sp. nov. highlights the underestimated diversity of high-elevation forests in southwestern China and further emphasizes the importance of integrative taxonomy in revealing cryptic lineages within *Scincella*. Phylogenetic analyses based on concatenated mitochondrial sequences recovered the Lincang population as a distinct phylogenetic lineage, sister to the *Scincella reevesii* species group (including *S. ochracea*, *S. ouboteri*, and *S. reevesii*). The new lineage further differs from its closest relatives by substantial genetic divergence, with ≥ 6.3% in *16S* and ≥ 16.6% in *CO1*. Together with consistent diagnostic morphological differences, these results robustly support the recognition of the Lincang population as a new species.

One of the most noteworthy findings of the present study concerns the incongruence between the phylogenetic placement of the new species and its morphology, which partially contradicts the formal diagnosis of the genus *Scincella*. Phylogenetically, the new species is unequivocally nested within *Scincella*. However, it exhibits a striking morphological peculiarity: the complete absence of a transparent palpebral disc on the lower eyelid. In skinks, the palpebral disc (or central disc, or "window") refers to a large, approximately circular or elliptical, semi-transparent scale on the lower eyelid, formed by the fusion and specialization of some lower palpebrals in some species with movable eyelids (Zhao et al. 1999; Zhao 2003). Historically, eyelid mobility and the presence or absence of a transparent palpebral disc have been regarded as taxonomically important characters in skink systematics and were frequently used to delimit skink genera, including *Scincella* (palpebral disc always present) and *Sphenomorphus* Fitzinger, 1843 (palpebral disc absent) (Ouboter 1986; Linkem et al. 2011; Nguyen 2011). Under this traditional framework, the absence of a palpebral disc might have suggested placement of the new species outside of the genus *Scincella*. Recent integrative taxonomic studies, however, increasingly question the stability of this character as a generic diagnostic feature (e.g., Mirza et al. 2022; Bragin et al. 2024). Accumulating evidence indicates that eyelid morphology may evolve repeatedly and independently within lineages and therefore may not reliably reflect deep phylogenetic relationships. Rather, variation in palpebral disc development appears to reflect the homoplastic evolution of this character. A recent example is

Figure 8. Habitat and field observations of *Scincella verecunda* sp. nov. **A.** Macrohabitat of the new species in Linxiang, Lincang, Yunnan, China; **B–C.** Microhabitat of the new species; **D.** *Scincella verecunda* sp. nov. in life, *in situ*. Photographs by J.C. Liu.

provided by the expanded circumscription of *Ablepharus* Fitzinger in Lichtenstein, 1823, which now incorporates the former genera *Himalblepharus* Eremchenko, 1987 (with movable eyelids and palpebral disc) and *Asymblepharus* Eremtschenko & Szczerbak, 1980 (with partially fused eyelids), despite substantial interspecific variation in eyelid morphology (Mirza et al. 2022; Bragin et al. 2024, 2025c). Molecular evidence clearly demonstrates that such variation does not correspond to genus-level boundaries and may be rather connected to species ecology. Our finding provides additional evidence that eyelid morphology is evolutionarily labile in scincid lizards and should be used with caution in higher-level taxonomy. The discovery of *Scincella verecunda* sp. nov. provides further evidence that the genus *Scincella* may represent a similar evolutionary scenario, suggesting that eyelid morphology could change multiple times during the evolution of this group and thus that it is unlikely to constitute a stable generic synapomorphy for the genus. Consequently, the current circumscription of *Scincella* may require re-evaluation in light of broader sampling and integrative taxonomic and phylogenetic approaches. Future studies incorporating denser taxon sampling, multilocus genomic data, and detailed comparative morphology will be essential to reassess the taxonomic boundaries of the genus.

In contrast to its closest relatives, which primarily occupy lowland or mid-elevation habitats, the new species appears to be restricted to high-elevation forests above 2,000 m a.s.l. Specifically, *Scincella ouboteri* inhabits limestone karst forests at approximately 400 m a.s.l., and *S. ochracea* occurs in grassland and shrub habitats at 500–600 m a.s.l., whereas *S. reevesii* is mainly associated with lowland environments below 1,500 m a.s.l. (Bourret 1937; Zhao et al. 1999; Chen et al. 2001; Pham et al. 2015; Neang et al. 2018; this study). This pronounced elevation and ecological segregation suggests that mon-

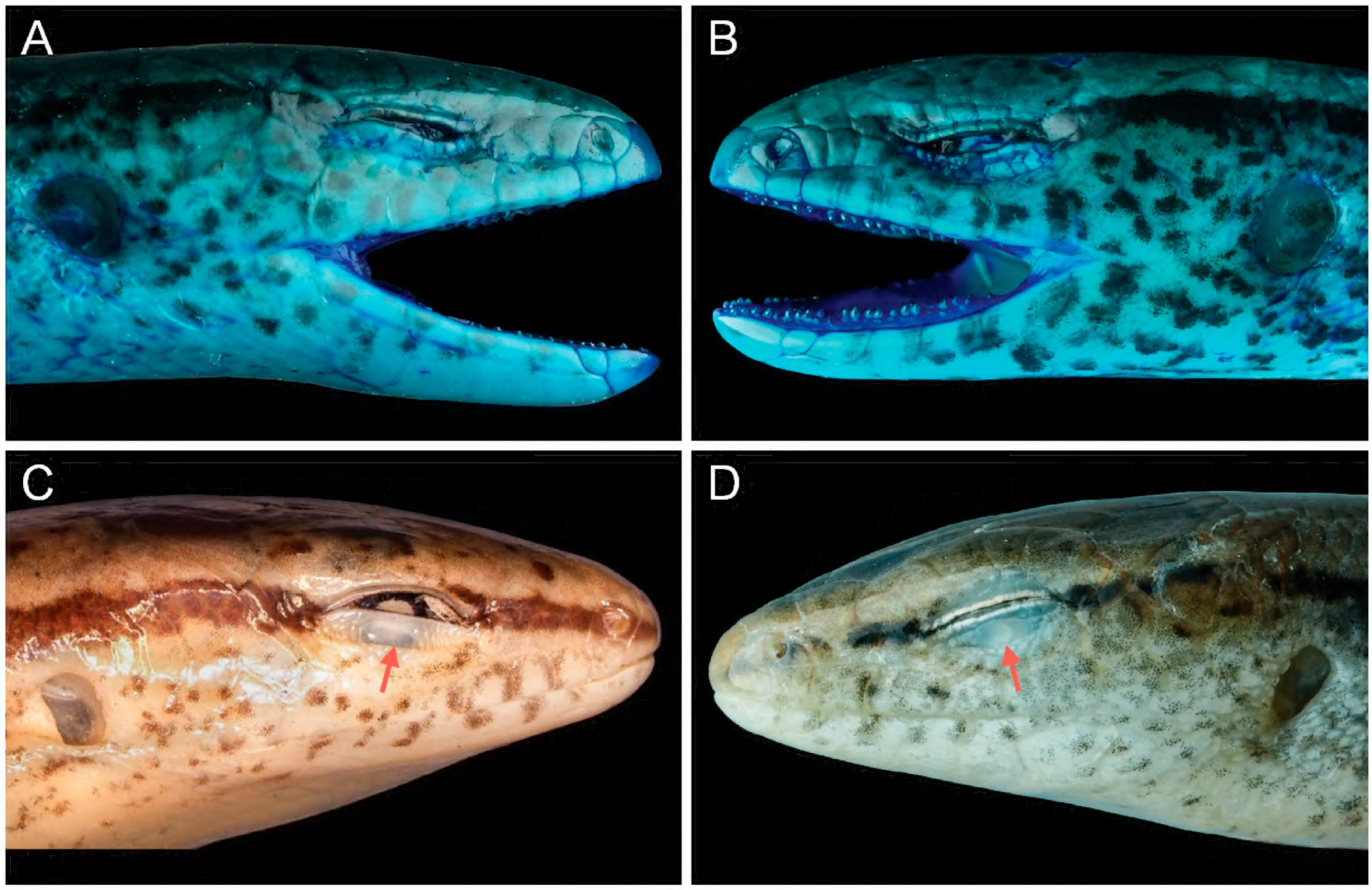

Figure 9. Comparison of lateral head views of *Scincella verecunda* sp. nov. (**A, B**), *S. ouboteri* (**C**), and *S. reevesii* (**D**). (**A**) QHU R2025058, holotype of *Scincella verecunda* sp. nov.; (**B**) QHU R2025059, paratype of *Scincella verecunda* sp. nov.; (**C**) IEBR 5042, holotype of *S. ouboteri*; (**D**) LFR 2025093, *S. reevesii* from Jinxiu, Guangxi ZAR, China. Red arrows in (**C**) and (**D**) indicate the palpebral disc. Photographs by Y.H. Xu (**A, B, D**) and reproduced from Pham et al. (2024) (**C**).

tane pine forests may function as isolated refugia ("sky islands"), facilitating local diversification and endemism.

Southwestern Yunnan lies at the biogeographic crossroads between the spurs of the eastern Himalaya (the Hengduan Mountains) and the mountains of northern Indochina. Overall, this region is characterized by complex topography, pronounced elevational gradients, and high levels of endemism. Such montane landscapes likely promote population isolation and lineage diversification in small ground-dwelling skinks, as demonstrated by recent discoveries of narrowly distributed *Scincella* species across the Hengduan Mountains region (see Xing and Ree 2017; Liu et al. 2026). This pattern suggests that localized orographic complexity may play a key role in driving cryptic diversification within the genus *Scincella*.

With the description of *Scincella verecunda* sp. nov., the number of *Scincella* species recorded from China increases to 19, of which five species occur in Yunnan Province, namely *Scincella verecunda* sp. nov., *S. barbouri*, *S. doriae*, *S. fansipanensis*, and *S. monticola* (Xu et al. 2025c; Liu et al. 2026). This finding further highlights southwestern China as an important center of diversification for *Scincella*. Given the apparent restriction of the new species to high-elevation pine forests and the limited number of known localities, additional field surveys are urgently needed to clarify its distribution, population status, and conservation requirements.

Acknowledgments

We sincerely thank Dr. Shuo Qi (SYS, China) and Dr. Bo Cai (CIB, China) for their constructive comments and valuable suggestions, which greatly improved the quality of this manuscript. This research was funded by the National Natural Science Foundation of China [32301325]; the Science and Technology Projects of Xizang Autonomous Region, China [XZ202501ZY0018]; and the Russian Science Foundation (RSF grant N° 22-14-00037-P, for supporting the work of N.A. Poyarkov, data analysis).

References

Akaike H (1973) Information theory and an extension of the maximum likelihood principle. In: Petrov BN, Csáki F (Eds) Second International Symposium on Information Theory, Tsahkadsor, Armenia, USSR. Akadémiai Kiadó, Budapest, 267–281. https://doi.org/10.1007/978-1-4612-1694-0_15

Akaike H (1974) A new look at the statistical model identification. IEEE Transactions on Automatic Control 19(6): 716–723. https://doi.org/10.1109/TAC.1974.1100705

Barbour T (1927) A new lizard from China. Copeia 165: 95.

Boulenger GA (1887) An account of the reptiles and batrachians obtained in Tenasserim by M. L. Fea, of the Genoa Civic Museum.

Annali del Museo Civico di Storia Naturale di Genova, Serie 2(5): 474–486.

Bourret R (1937) Notes herpétologiques sur l'Indochine française. XII. Les lézards de la collection du Laboratoire des Sciences Naturelles de l'Université. Bulletin général de l' Instruction Publique, Hanoi 9: 1–39.

Bourret R (2009) Les Lezards de L'Indochine. Edition Chimaira, Frankfurt am Main, 624 pp.

Bragin AM, Litvinchuk SN, Borkin LJ, Melnikov DA, Skorinov DV, Jablonski D, Masroor R, Lalremsanga HT, Mirza ZA, Dufresnes C, Poyarkov NA (2024) Hidden on the roof of the world: Mitochondrial data reveals exceptional genetic diversity of Himalayan ablepharine skinks (Reptilia: Scincidae). Russian Journal of Herpetology 31(6): 351–368. https://doi.org/10.30906/1026-2296-2024-31-6-351-368

Bragin AM, Zenin ES, Dang CH, Dinh VAT, Nguyen TV, Poyarkov NA (2025a) A new mountain species of the genus *Scincella* Mittleman, 1950 (Squamata: Scincidae) from Ha Giang Province, northern Vietnam. Zootaxa 4868(3): 423–434. https://doi.org/10.11646/zootaxa.5636.2.1

Bragin AM, Zenin ES, Le SX, Nguyen DT, Nguyen TV, Poyarkov NA (2025b) Gold of the highlands: a new ground skink (Squamata: Scincidae: *Scincella* Mittleman) from southern Vietnam. Zootaxa 5701(3): 247–291. https://doi.org/10.11646/zootaxa.5701.3.2

Bragin AM, Decemson H, Lalremsanga HT, Mirza ZA, Poyarkov NA (2025c) A new species of Himalayan skink of the genus *Ablepharus* (Squamata: Scincidae). Salamandra 61(4): 373–394. https://doi.org/10.5281/zenodo.17482376

Burland TG (2000) DNASTAR's Lasergene sequence analysis software. Methods Molecular Biology 132: 71–91. https://doi.org/10.1385/1-59259-192-2:71

Chen SL, Hikida T, Han SH, Shim JH, Oh HS, Ota H (2001) Taxonomic status of the Korean populations of the genus *Scincella* (Squamata: Scincidae). Journal of Herpetology 35(1): 122–129. https://doi.org/10.2307/1566034

Darevsky IS, Nguyen SV (1983) New and little known lizard species from Vietnam. Zoologitchesky Zhurnal 62: 1827–1837. [in Russian]

Darevsky IS, Orlov NL (1997) A new genus and species of scincid lizards from Vietnam: the first Asiatic skink with double rows of basal subdigital pads. Journal of Herpetology 31(3): 323–326. https://doi.org/10.2307/1565659

Darevsky IS, Orlov NL, Ho TC (2004) Two new lygosomine skinks of the genus *Sphenomorphus* Fitzinger, 1843 (Sauria, Scincidae) from northern Vietnam. Russian Journal of Herpetology 11: 111–120.

Darko YA, Voss O, Uetz P (2022) A dictionary of abbreviations used in reptile descriptions. Zootaxa 5219(5): 421–432. https://doi.org/10.11646/zootaxa.5219.5.2

Edgar RC (2004) MUSCLE: Multiple sequence alignment with high accuracy and high throughput. Nucleic Acids Research 32(5): 1792–1797. https://doi.org/10.1093/nar/gkh340

Gray JE (1838) Catalogue of the slender-tongued saurians, with descriptions of many new genera and species. Annals and Magazine of Natural History 2(10): 287–293. https://doi.org/10.1080/00222933809496676

Greer AE (1974) The generic relationships of the scincid lizard genus *Leiolopisma* and its relatives. Australian Journal of Zoology (Suppl. Ser. 31): 1–67. https://doi.org/10.1071/AJZS031

Greer AE, Shea G (2003) Secondary temporal scale overlap pattern: A character of possible broad systematics Importance in Sphenomorphine skinks. Journal of Herpetology 37(3): 545–549. https://doi.org/10.1670/104-02N

Günther A (1896) Report on the collections of reptiles, batrachians and fishes made by Messrs. Potanin and Berezowski in the Chinese provinces Kansu and Sze-chuen. Annuaire du Musee Zoologique de l'Academie des Sciences de St. Petersbourg 1: 199–219. https://doi.org/10.1080/00222939608680365

Hoang DT, Chernomor O, Haeseler AV, Minh BQ, Vinh LS (2018) UFBoot2: Improving the ultrafast bootstrap approximation. Molecular Biology and Evolution 35(2): 518–522. https://doi.org/10.1093/molbev/msx281

Huelsenbeck JP, Ronquist F, Nielsen R, Bollback JP (2001) Bayesian inference of phylogeny and its impact on evolutionary biology. Science 294: 2310–2314. https://doi.org/10.1126/science.1065889

Inger RF, Zhao EM, Shaffer HB, Wu G (1990) Report on a collection of amphibians and reptiles from Sichuan, China. Fieldiana: Zoology 58: 1–24. https://doi.org/10.5962/bhl.title.3126

IUCN (2026) The IUCN Red List of Threatened Species. 2020. Version 2024-2. https://www.iucnredlist.org/ [accessed 15 February 2026]

Jia RW, Gao ZY, Huang JJ, Ren JL, Jiang K, Li DY, Li JT (2023) A new species of the genus *Scincella* Mittleman, 1950 (Squamata: Scincidae) from Sichuan Province, Southwest China, with a diagnostic key of *Scincella* species in China. Asian Herpetological Research 14(1): 24–40. https://doi.org/10.3724/ahr.2095-0357.2024.0016

Jia RW, Gao ZY, Wu DH, Ren JL, Jiang DC, Wu W (2024) A new species of the genus *Scincella* Mittleman, 1950 (Squamata: Scincidae) from Sichuan Province, Southwest China. Asian Herpetological Research 15(2): 115–129. https://doi.org/10.3724/ahr.2095-0357.2024.0016

Jia RW, Gao ZY, Wu DH, Wang GQ, Liu G, Liu M, Jiang K, Jiang DC, Ren JL, Li JT (2025) Hidden Urban Biodiversity: A new species of the genus *Scincella* Mittleman, 1950 (Squamata: Scincidae) from Chengdu, Sichuan Province, Southwest China. Animals 15(2): 232. https://doi.org/10.3390/ani15020232

Kalyaanamoorthy S, Minh BQ, Wong TKF, Haeseler AV, Jermiin LS (2017) ModelFinder: fast model selection for accurate phylogenetic estimates. Nature Methods 14(6): 587–589. https://doi.org/10.1038/nmeth.4285

Kocher TD, Thomas WK, Meyer A, Edwards SV, Pääbo S, Villablanca FX, Wilson AC (1989) Dynamics of mitochondrial DNA evolution in animals: amplification and sequencing with conserved primers. Proceedings of the National Academy of Sciences 86(16): 6196–6200. https://doi.org/10.1073/pnas.86.16.6196

Koizumi Y, Ota H, Hikida T (2022) A new species of the genus *Scincella* (Squamata: Scincidae) from Yonagunijima Island, Southern Ryukyus, Japan. Zootaxa 5128: 61–83. https://doi.org/10.11646/zootaxa.5128.1.3

Kumar S, Stecher G, Li M, Knyaz C, Tamura K (2018) MEGA X: Molecular Evolutionary Genetics Analysis across computing platforms. Molecular Biology and Evolution 35: 1547–1549. https://doi.org/10.1093/molbev/msy096

Linkem CW, Diesmos AC, Brown RM (2011) Molecular systematics of the Philippine forest skinks (Squamata: Scincidae: *Sphenomorphus*): testing morphological hypotheses of interspecific relationships. Zoological Journal of the Linnean Society 163(4): 1217–1243. https://doi.org/10.1111/j.1096-3642.2011.00747.x

Liu F, Pu HL, Tan SW, Chen JH, Lyu B, Shu GC, Wu YY, Dong BJ, Guo P (2026) A new species of the genus *Scincella* Mittleman, 1950 (Squamata: Scincidae) from the Hengduan Mountains, Sichuan Province, western China. Animals 16: 592. https://doi.org/10.3390/ani16040592

Mirza ZA, Bragin AM, Bhosale H, Gowande GG, Patel H, Poyarkov NA (2022) A new ancient lineage of ablepharine skinks (Sauria: Scincidae) from eastern Himalayas with notes on origin and systematics of the group. PeerJ 10: e12800. https://doi.org/10.7717/peerj.12800

Mittleman MB (1950) The generic status of *Scincus lateralis* Say, 1823. Herpetologica 6: 17–20.

Nagy ZT, Sonet G, Glaw F, Vences M (2012) First large-scale DNA barcoding assessment of reptiles in the biodiversity hotspot of Madagascar, based on newly designed *COI* primers. PLoS ONE 7(3): e34506. https://doi.org/10.1371/journal.pone.0034506

Neang T, Chan S, Poyarkov NA (2018) A new species of smooth skink (Squamata: Scincidae: *Scincella*) from Cambodia. Zoological Research 39(3): 220–240. https://doi.org/10.24272/j.issn.2095-8137.2018.008

Nguyen LT, Schmidt HA, Haeseler AV, Minh BQ (2015) IQ-TREE: A fast and effective stochastic algorithm for estimating maximum likelihood phylogenies. Molecular Biology and Evolution 32(1): 268–274. https://doi.org/10.1093/molbev/msu300

Nguyen SN, Nguyen VDH, Nguyen LT, Murphy RW (2019) A new skink of the genus *Scincella* Mittleman, 1950 (Squamata: Scincidae) from Ba Den Mountain, Tay Ninh Province, southern Vietnam. Zootaxa 4648(2): 273–286. https://doi.org/10.11646/zootaxa.4648.2.4

Nguyen SN, Nguyen VDH, Nguyen LT, Murphy RW (2020) A new skink of the genus *Scincella* Mittleman, 1950 (Squamata: Scincidae) from southern Vietnam. Zootaxa 4668(3): 423–434. https://doi.org/10.11646/zootaxa.4868.3.6

Nguyen SN, Nguyen LT, Le MV, Nguyen VDH, Phan KD, Vo TDH, Murphy RW, Che J (2025) Two new skinks of the genus *Scincella* Mittleman, 1950 (Squamata: Scincidae) from southern Vietnam. European Journal of Taxonomy 989: 266–288. https://doi.org/10.5852/ejt.2025.989.2899

Nguyen TQ, Ananjeva NB, Orlov NL, Rybaltovsky E, Böhme W (2010a) A new species of the genus *Scincella* Mittleman, 1950 (Squamata: Scincidae) from Vietnam. Russian Journal of Herpetology 17(4): 269–274. https://doi.org/10.25225/fozo.v59.i2.a6.2010

Nguyen TQ, Nguyen SV, Böhme W, Ziegler T (2010b) A new species of *Scincella* (Squamata: Scincidae) from Vietnam. Folia Zoologica 59(2): 115–121. https://doi.org/10.25225/fozo.v59.i2.a6.2010

Nguyen TQ, Schmitz A, Nguyen TT, Orlov NL, Böhme W, Ziegler T (2011) Review of the genus *Sphenomorphus* Fitzinger, 1843 (Squamata: Sauria: Scincidae) in Vietnam, with description of a new species from Northern Vietnam and Southern China and the first record of *Sphenomorphus mimicus* Taylor, 1962 from Vietnam. Journal of Herpetology 45(2): 145–154. https://doi.org/10.1670/09-068.1

Nguyen VDH, Tran TG, Hoang HD, Luong HQ, Ton BN, Laumanns M, Nguyen MA, Nguyen TTP, Orlov NL (2024) The first record of *Scincella nigrofasciata* Neang, Chan & Poyarkov, 2018 (Reptile, Squamata, Scincidae) in Lava Caves in Dak Nong UNESCO Global Geopark, Vietnam. Russian Journal of Herpetology 31(6): 369–378. https://doi.org/10.30906/1026-2296-2024-31-6-369-378

Okabe S, Motokawa M, Koizumi Y, Nguyen TQ, Nguyen TT, Bui HT (2024) A new species of the genus *Scincella* (Squamata: Scincidae) from Mount Fansipan, Hoang Lien Son Range, northwestern Vietnam. Zootaxa 5537(3): 407–423. https://doi.org/10.11646/zootaxa.5537.3.7

Ouboter PE (1986) A revision of the genus *Scincella* (Reptilia: Sauria: Scincidae) of Asia, with some notes on its evolution. Zoologische Verhandelingen 229: 1–66.

Pham AV, Le DT, Nguyen SLH, Ziegler T, Nguyen TQ (2015) New provincial records of skinks (Squamata: Scincidae) from northwestern Vietnam. Biodiversity Data Journal 3: e4284. https://doi.org/10.3897/BDJ.3.e4284

Pham AV, Pham CT, Le MD, Ngo HN, Ziegler T, Nguyen TQ (2024) A new skink of the genus *Scincella* Mittleman, 1950 (Squamata: Scincidae) from Hoa Binh Province, northern Vietnam. Zootaxa 5428(1): 91–106. https://doi.org/10.11646/zootaxa.5428.1.4

Pham AV, Ziegler T, Pham CT, Hoang TN, Ngo HT, Le MD (2025) A new skink of the genus *Scincella* Mittleman, 1950 (Squamata, Scincidae) from Son La Province, northwestern Vietnam. ZooKeys 1226: 319–337. https://doi.org/10.3897/zookeys.1226.139655

Rambaut A (2018) FigTree v1.4.4. http://tree.bio.ed.ac.uk/software/figtree/ [accessed 10 April 2025]

Ronquist F, Teslenko M, Van Der Mark P, Ayres DL, Darling A, Höhna S, Larget B, Liu L, Suchard MA, Huelsenbeck JP (2012) MrBayes 3.2: Efficient Bayesian phylogenetic inference and model choice across a large model space. Systematic Biology 61: 539–542. https://doi.org/10.1093/sysbio/sys029

Schmidt KP (1927) Notes on Chinese reptiles. Bulletin of the American Museum of Natural History 54: 467–551.

Smith MA (1935) The Fauna of British India, including Ceylon and Burma. Reptilia and Amphibia. Vol. II. Sauria. Taylor and Francis, London, 440 pp.

Stejneger L (1925) Description of a new scincid lizard and a new burrowing from China. Journal of the Washington Academy of Sciences 15: 150–152.

Stephane G, Jean-franc OD, Vincent L, Maria A, Wim H, And OG (2010) New algorithms and methods to estimate Maximum-likelihood phylogenies: Assessing the performance of PhyML 3.0. Systematic Biology 59(3): 307–321. https://doi.org/10.1093/sysbio/syq010

Taylor EH (1963) The lizards of Thailand. University of Kansas Science Bulletin 44: 687–1077

Uetz P, Freed P, Aguilar R, Reyes F, Kudera J, Hošek J [Eds] (2026) The Reptile Database. http://www.reptile-database.org/ [accessed 11 February 2026]

van Denburgh J (1912) Concerning certain species of reptiles and amphibians from China, Japan, the Loo Choo Islands, and Formosa. Proceedings of the California Academy of Science 4(3): 187–258.

Wang YZ, Zhao EM (1986) Studies on Chinese species of *Scincella* (Scincidae, Sauria). Acta Herpetologica Sinica 5: 267–277. [in Chinese]

Xu YH, Gong ZH, Nguyen TV, Deng JD, Bragin AM, Weng SY, Zhang TR, Poyarkov NA, Peng LP (2025a) A new species of the genus *Scincella* Mittleman, 1950 (Squamata, Scincidae) from Guizhou Province, southwest China. ZooKeys 1258: 9–33. https://doi.org/10.3897/zookeys.1258.161382

Xu YH, Liao CC, Poyarkov NA, Weng SY, Deng JD, Bragin A, Zhang TR, Nguyen TV, Peng LF (2025b) First record of *Scincella fansipanensis* Okabe, Motokawa, Koizumi, Nguyen, Nguyen & Bui, 2024 (Squamata: Scincidae) from China. Biodiversity Data Journal 13: e161782. https://doi.org/10.3897/BDJ.13.e161782

Xu YH, Weng SY, Poyarkov NA, Zhang TR, Li ZY, Deng JD, Peng LF (2025c) Discovery of a new skink of the genus *Scincella* Mittleman, 1950 (Squamata, Scincidae) from Guizhou Province, China. Zoosystematics and Evolution 101(4): 1495–1511. https://doi.org/10.3897/zse.101.157713

Xing Y, Ree RH (2017) Uplift-driven diversification in the Hengduan Mountains, a temperate biodiversity hotspot. Proceedings of the National Academy of Sciences of the United States of America 114(17): E3444–E3451. https://doi.org/10.1073/pnas.1616063114 (2017).

Zhang D, Gao FL, Jakovlić I, Zou H, Zhang J, Li WX, Wang GT (2020) PhyloSuite: an integrated and scalable desktop platform for streamlined molecular sequence data management and evolutionary phylogenetics studies. Molecular Ecology Resources 20(1): 348–355. https://doi.org/10.1111/1755-0998.13096

Zhao EM (2003) The Colour Hand Book of the Reptiles of Sichuan. China Forestry Publishing House, Beijing, 292 pp. [in Chinese]

Zhao EM, Zhao K, Zhou K (1999) Fauna Sinica. Reptilia, Vol. 2, Squamata, Lacertilia. Science Press, Beijing, 312–336. [in Chinese]

Zhao EM, Huang KC (1982) A survey of amphibians and reptiles in Liaoning Province. Acta Herpetologica Sinica 1: 1–23. [in Chinese]

Supplementary material 1

Additional tables

Authors: Yuhao Xu, Tan Van Nguyen, Jundong Deng, Tierui Zhang, Fanyue Sun, Junchang Liu, Nikolay A. Poyarkov, Lifang Peng

Data type: zip

Explanation note: **table S1.** GenBank accession numbers, localities, and voucher information for all specimens used in this study. **table S2.** Uncorrected *p*-distances (%) of the *16S* gene among species of *Scincella* used in this study. "/" indicates not available. **table S3.** Uncorrected *p*-distances (%) of the *CO1* gene among species of *Scincella* used in this study. "/" indicates not available.

Copyright notice: This dataset is made available under the Open Database License (http://opendatacommons.org/licenses/odbl/1.0/). The Open Database License (ODbL) is a license agreement intended to allow users to freely share, modify, and use this Dataset while maintaining this same freedom for others, provided that the original source and author(s) are credited.

Link: https://doi.org/10.3897/herpetozoa.39.e188979.suppl1